

An Artificial Chaperone Serves a Dual Role in Regulating the Assembly of Peptides through Phase Separation

Wang Li¹, Yang Zhou¹, Sheng He¹, Congsen Wang¹, Peichen Shi¹, Suixu Li¹, Xinchang Wang¹, Liulin Yang¹, Xiao-Yu Cao¹, and Zhong-Qun Tian¹

¹Xiamen University

September 28, 2023

Abstract

In biological systems, molecular assembly primarily relies on the assistance of molecular chaperones. Inspired by nature, strategies like ‘chaperone-assisted assembly’ and ‘catalyzed assembly’ have been proposed towards the sophisticated control of molecular assembly. Nonetheless, significant challenges remain in the rational design of such systems, calling for a deep understanding of underlying principles. Herein, we demonstrate an artificial chaperone serves a dual role, i.e. catalyst in low dosages and inhibitor in high dosages, in regulating the supramolecular polymerization of peptides. Low dosages of carboxymethyl cellulose, as the chaperones, catalyse the assembly of A β 16-22 peptides into fibrils through multi-step phase separation, while high dosages trap the peptides into coacervate intermediates and therefore inhibit the fibrillation. Consequently, the quantity of chaperone does not follow the intuition that ‘more is better’ for catalyzing assembly, but instead has an optimal molar ratio. Investigation reveals that the interplay and evolution of electrostatic and hydrophobic interactions between chaperones and peptides are the keys to achieving these processes. This study provides insights into the multifaceted roles artificial chaperones may play in a dosage-dependent manner, and enriches the toolkit for efficient and controllable construction of complex assembly systems.

An Artificial Chaperone Serves a Dual Role in Regulating the Assembly of Peptides through Phase Separation

Wang Li¹, Yang Zhou¹, Sheng He¹, Congsen Wang¹, Peichen Shi¹, Suixu Li¹, Xinchang Wang², Liulin Yang^{1*}, Xiaoyu Cao^{1*}, and Zhongqun Tian¹

W. Li, Y. Zhou, S. He, C. S. Wang, P. C. Shi, S. X. Li, Prof. L. L. Yang, Prof. X. Y. Cao, and Prof. Z. Q. Tian

¹State Key Laboratory of Physical Chemistry of Solid Surface, Key Laboratory of Chemical Biology of Fujian Province, Collaborative Innovation Center of Chemistry for Energy Materials (iChEM), Innovation Laboratory for Sciences and Technologies of Energy Materials of Fujian Province (IKKEM), College of Chemistry and Chemical Engineering, Xiamen University, Xiamen 361005, P. R. China

E-mail: llyang@xmu.edu.cn, xcao@xmu.edu.cn

Prof. X. C. Wang² School of Electronic Science and Engineering (National Model Microelectronics College), Xiamen University, Xiamen 361005, P. R. China

Keywords : artificial chaperone, catassembly, supramolecular polymerization, peptide assembly

Abstract: In biological systems, molecular assembly primarily relies on the assistance of molecular chaperones. Inspired by nature, strategies like ‘chaperone-assisted assembly’ and ‘catalyzed assembly’ have been proposed towards the sophisticated control of molecular assembly. Nonetheless, significant challenges remain in the rational design of such systems, calling for a deep understanding of underlying principles. Herein,

we demonstrate an artificial chaperone serves a dual role, i.e. catalyst in low dosages and inhibitor in high dosages, in regulating the supramolecular polymerization of peptides. Low dosages of carboxymethyl cellulose, as the chaperones, catalyse the assembly of A β ₁₆₋₂₂ peptides into fibrils through multi-step phase separation, while high dosages trap the peptides into coacervate intermediates and therefore inhibit the fibrillation. Consequently, the quantity of chaperone does not follow the intuition that ‘more is better’ for catalyzing assembly, but instead has an optimal molar ratio. Investigation reveals that the interplay and evolution of electrostatic and hydrophobic interactions between chaperones and peptides are the keys to achieving these processes. This study provides insights into the multifaceted roles artificial chaperones may play in a dosage-dependent manner, and enriches the toolkit for efficient and controllable construction of complex assembly systems.

1. Introduction

The pathway complexity of supramolecular polymerization, along with its high sensitivity to solvents, additives, impurities, and environmental conditions, poses significant challenges for thermodynamic and kinetic regulations.^[1-13] In recent years, strategies have been developed to trigger supramolecular polymerization, select polymerization pathways, and control polymer structures. These are represented by (seeded) living supramolecular polymerization,^[14-18] fuel-driven supramolecular polymerization,^[19, 20] supramolecular interfacial polymerization,^[21] controlled release monomers from macromolecules,^[22] and using external stimuli.

Assembly assisted by molecular chaperones has been recognized as an efficient strategy in biological systems, however, less explored in supramolecular polymerizations. Chaperones are well known to assist in the correct folding and assembly of proteins. ATP-independent chaperones often act as ‘holdases’,^[23] they bind to misfolded proteins to prevent their further aggregation. Examples of artificial chaperones based on similar mechanisms have been developed for regulating protein folding.^[24] Recently, this strategy was employed in controlling the supramolecular polymerization of squaraine dye monomers, in which the monomer was kinetically trapped by a macrocycle chaperone, and the living supramolecular polymerization was then triggered by adding an initiator to remove the chaperone.^[25]

Some ATP-independent molecular chaperones can play the role of ‘foldases’, assisting in the folding of substrate proteins after binding.^[23, 26-29] Achieving this process requires a loose binding between the molecular chaperone and the protein, allowing the protein enough flexibility to explore its conformation space.^[23] Once the folded protein is formed, the binding affinity between the protein and the molecular chaperone decreases, resulting in the regeneration of the chaperone.^[27, 30] Such a chaperone-mediated folding-while-bound mechanism was employed in artificial chaperone systems, which realizes the renaturation of proteins.^[31-34] Inspired by these catalytic molecular chaperones as well as the catalytic chemistry, a concept of catassembly^[35, 36] had been proposed as an efficient assisted assembly strategy. As a prove of concept, polyhedral molecular cages were demonstrated to serve as chaperones to enantioselective catalyze the supramolecular polymerization of a porphyrin monomer.^[37] The molecular cages eventually dissociate from the supramolecular polymer through phase separation.

As mentioned above, the content of additives can significantly influence assembly pathways, highlighting the intricate complexity in regulating assembly kinetics. This has propelled us to explore the impact of stoichiometry of chaperones as additives on the kinetics of supramolecular polymerizations. Here, we report an artificial chaperone serves a dual role in regulating peptide assembly in a dosage-dependent manner, i.e. catalyzing assembly at low dosages while inhibiting assembly at high dosages. As shown in scheme 1, carboxymethyl cellulose (CMD) was employed as a molecular chaperone to regulate the assembly of A β ₁₆₋₂₂ peptide (KLVFFAE, abbreviated as KE). CMD initially enriched the peptide monomers and formed coacervate droplets through liquid-liquid phase separation (LLPS). Subsequently, at different CMD dosages, CMD played two opposite roles within the coacervates. When the dosage of CMD was low, coacervates facilitated the nucleation of peptides, and further fibrillation by desolvation and releasing CMD through phase separation. In contrast, CMD with higher dosage trapped the system in the coacervate state, slowed down and even inhibited the peptide fibrillation. We believe this phenomenon where a molecular chaperone

plays opposite roles at different dosages is likely widespread. Investigating the underlying mechanism can help us gain a deeper understanding in chaperone-assisted molecular assembly and develop new assembly strategies, e.g. catassembly.

2 . Results and Discussion

2.1.Low dosage of CMD promoted the peptide assembly

The KE monomer was initially trapped into a random coil conformation in the aqueous solution at pH 4.25 (Figure S1). The addition of low dosage of CMD (< 1 mol% of KE, calculated in moles of glucose units) triggered the conformational transition of KE from α -helix to β -strand and subsequently the assembly into fibrils (Figure 1). The conformational transition of the peptide was demonstrated by the circular dichroism (CD) spectra, in which the peak at 215 nm gradually diminished, and the spectra eventually became a single peak with only the β -strand conformation (Figure 1B).^[38] Meanwhile, the supramolecular polymerization of β -strand KE was evidenced by a gradual increase in the emission at 482 nm using a ThT fluorescence probe^[39] (Figure 1C), and also the images of transmission electron microscopy (TEM) (Figure S2) sampled at different time points. Some droplet-like coacervates in the early-stage samples were observed under TEM, suggesting that KE may complex with CMD in solution and undergo LLPS (Figure 1A). The phenomenon of LLPS often originates from the complexation of oppositely charged polyelectrolytes, such as nucleic acids and proteins, in aqueous solution, which leads to phase separation and the formation of coacervate droplets. Since CMD molecules were negatively charged, while KE molecules were positively charged under the experimental conditions (Figure S3A), it is plausible that they formed coacervate droplets through electrostatic interactions and facilitate KE fibrillation. In contrast, a neutral polysaccharide, dextran, which has the same backbone structure as CMD but without carboxyl groups (Figure S3B), had no effect on KE assembly (Figure S4).

Confocal laser scanning microscopy (CLSM) provided further insight into the LLPS and fibrillation process (Figure 2, Movie S1). The CMD and KE were labelled by fluorescein isothiocyanate (FITC, emitting green fluorescence) and rhodamine B (RhoB, emitting red fluorescence), respectively. In the initial stages, yellowish-green spherical coacervates were observed, and fluorescence imaging analyses^[40, 41] indicated that these coacervates were enriched in CMD and KE (Figure 2A). Subsequently, protofibrils generated within these droplets, and then elongated into fibrils that interconnect multiple droplets (Figure 2B-D). As the droplet diminished over time, a large number of mature fibrils were eventually obtained (Figure S5).^[42] These results indicate that CMD and KE can form coacervates through LLPS, and these metastable coacervates then function as nucleation centers to promote the fibrillation of the peptide.

2.2. Highdosage of CMD inhibited the peptide assembly

However, the formation of coacervates did not necessarily promote peptide fibrillation. In contrast, large amounts of CMD inhibited KE fibrillation, despite forming coacervates with KE (Figure 3). By adding 5 equivalents of CMD, a notable inhibition effect on KE fibrillation was observed both visually and from the fluorescence kinetic data (Figures 3A and 3B). Upon the introduction of 50 equivalents of CMD, the solution remained consistently transparent and devoid of fibril formation. Although coacervates were still found, these entities remained stabilized and refrained from transitioning into fibrils (Figure 3C). CD spectra showed that the peptides maintained the initial random coil conformation instead of transitioning into the β -strand conformation (Figure S6). At this point, CMD plays a role similar to that of an inhibitor in molecular chaperones. These results indicate that although CMD tends to form coacervates with KE, whether the CMD acts as a promotor or inhibitor inside the coacervates is closely related to its molar ratio. Therefore, the intricate kinetic mechanisms behind this phenomenon necessitate a comprehensive investigation.

2.3. Low dosage of CMD catalyzed the assembly of KE through multi-step phase separation

To explore the mechanism of peptide fibrillation promoted by low dosage of CMD, a quantitative fluorescence analysis of selected regions using CLSM was carried out. As the fibrillation progressed, the red emission from the peptides gradually enhanced, whereas the green emission from CMD attenuated (Figure 4A-C and Movie S1). This phenomenon implies that while KE monomers were stacking into fibrils, CMD molecules

were progressively dissociating from KE monomers, eventually expelled from the coacervates. Furthermore, correlation analysis showed a low correlation between green and red signals at the end of assembly (Figure 4C). This finding signifies a tendency for the KE fibrils and CMD to undergo phase separation.

To gain deeper insights into the evolution of interaction between CMD and KE, time-dependent Förster resonance energy transfer (FRET) measurements were performed. CMD was labeled with FAM, while KE was labeled with Rhodamine B. When excited at 380 nm, the maximum emission of CMD-FAM and KE-RhoB peaked at 512 and 575 nm, respectively. After mixing the CMD-FAM and KE-RhoB solutions, the emission at 575 nm quickly increased in 15-20 s, accompanied by the emission at 512 nm declined (Figure 4D and 4F). In a control experiment, the excitation of dye molecules FAM could not induce the enhancement of the emission of KE-RhoB, verifying the FRET effect between CMD-FAM and KE-RhoB (Figure S7). This result indicated a fast association between CMD and peptides upon mixing, which triggered the FRET effect after the proximity of the two fluorescent groups. Subsequently, the emission at 575 nm started to attenuate, while the emission at 512 nm recovered in around 2 min (Figure 4E and 4F). We speculated that this corresponded to the process of KE monomers dissociating from CMD and assembling into fibrils. Due to the consumption of KE monomers and the phase separation of fibrils from CMD, the FRET signal gradually attenuated. This observation is in line with the findings from CLSM analysis.

The self-assembly of peptides often follows a non-classical nucleation-growth mechanism, where peptides first undergo LLPS to form coacervates, and then nucleate inside the coacervates and eventually generate fibrils.^[42] During this process, the stacking of peptide molecules involves a desolvation process, i.e. expelling the water molecules that interacting with the peptides.^[42, 43] In this research, since the participation of the polyelectrolyte CMD, the phase separation underwent at least two stages and was not just a desolvation process. First, CMD and KE formed coacervates mainly through electrostatic interactions, corresponding to the first stage of phase separation. Afterwards, KE molecules stacked with each other, while further expelling solvent water and hydrophilic CMD from the coacervates, representing the second stage of phase separation. The isothermal titration calorimetry (ITC) measurements (Figures S8 and S9) demonstrated that the assembly of KE chaperoned by CMD is entropy-driven, which supported this phase separation-mediated assembly process.^[44] Phase separation phenomena were also observed in other chaperone-assisted assembly systems, such as the departure of molecular cages through phase separation after inducing chiral supramolecular polymerization of porphyrins.^[37] Therefore, the CMD acted as an enzyme analogous that can catalyze the assembly of peptides.

Figure 5A illustrates the process of CMD-catalyzed KE assembly. When mixing, negatively charged CMD rapidly enriches positively charged KE molecules and forms coacervates through LLPS. These concentrated compartments facilitate KE molecules to adopt β -strand conformation and stack into nuclei, which further induces more KE monomers to transform into β -strand conformation and participate in assembly, eventually forming fibrils. The stacking of KE molecules drives their dissociation from CMD, prompting their assembly into fibrils and the consequent release of CMD. Reflecting on this, we have outlined the assembly equation of KE catalyzed by CMD (Figure 5B). This process is analogous to protein assembly catalyzed by non-ATP independent chaperones within biological systems. As we mentioned above, it requires a loose binding between the chaperone and the substrate, while the dissociation constant (K_D) between them should be at the millimolar level.^[23] In our research system, the K_D of KE and CMD is 1.30 mM as measured by the surface plasmon resonance technique (SPR) (Figure S10), which just meets the above requirements. The relatively high K_D value results in a continuous interplay of association and dissociation between CMD and KE peptides, facilitating the peptides to adjust conformation and assembly. In biological system, the binding affinity between molecular chaperones and products is often weaker than that with substrates, therefore prone to dissociation due to competitive binding.^[23] Here, the release of CMD should be driven by the competitive stacking of KE monomers that finally expel the CMD through phase separation.

2.4. Kinetic analysis of peptide assembly inhibited by high dosage of CMD

Based on the assembly equation in Figure 5B, we inferred that increasing the dosage of CMD, while facilitating the nucleation of KE, may subsequently inhibit the growth of nucleus. To validate this hypothesis,

we investigated the effect of CMD dosage on KE assembly kinetics by collecting kinetic data (Figure 6A) and fitting the data to a theoretical model (Details in the *SI, Theoretical Methods section*). Initially, the addition of CMD increased both the apparent nucleation and elongation rate constants. The lag time for the assembly of KE was significantly shortened. When 0.01 equivalent ($1 \mu\text{M}$) of CMD was added, the lag time was almost undetectable. However, as the CMD content continued to increase, a distinct decline manifested in the apparent elongation rate constant (k_E). Therefore, an optimal CMD amount at around 1 mol% (Figure 6B, Supporting Information Table S1) resulted the highest apparent polymerization rate constant (Figure S12). A similar result was obtained from kinetic data collected by CD spectroscopy (Figure S13). At high CMD content, KE monomers and nuclei associated with CMD at a higher probability. On one hand, this reduced the concentration of free KE monomers in the solution, and on the other, competitive binding from high dosage of CMD prevented the association of KE monomer and nuclei. This complex interplay ultimately resulted in a decrease of fibril growth rate constant.

The competitive binding from high dosage of CMD that inhibit the fibrillation was further verified by time-dependent FRET experiments (Figure S14). The addition of varying molar ratios of CMD-FAM to the KE-RhoB solution leads to a rapid decrease in the emission at 512 nm. The extent of the decrease in luminescence intensity corresponds to the amount of peptide monomers adsorbed by CMD-FAM. As the dosage of CMD-FAM increased, the extent of emission reduction correspondingly increased, until reaching a plateau due to the completely adsorption of the peptide (Figure 7A). As the fibrillation progressed, KE-RhoB monomers disassociated from CMD-FAM and assembled into fibrils, resulting in a gradual recovery of the emission at 512 nm and an attenuation of FRET signal. However, the extent of CMD-FAM dissociation from complexes correlated with the dosage of CMD-FAM (Figure 7B). Low dosage of CMD-FAM generated small number of nuclei, resulting in slow monomer consumption, and correspondingly slow recovery of emission at 512 nm. For high dosage of CMD-FAM that adsorbed the peptide completely, a less recovery of the emission at 512 nm was observed, indicating that the competitive binding of CMD-FAM hindered the assembly of peptide and the release of CMD-FAM.

As we have demonstrated in this work, artificial molecular chaperones can exert complex effects on the kinetics of supramolecular polymerization due to their dynamic and reversible interactions with substrates, intermediates, and products. According to the assembly equation we proposed (Figure 5B), excessive molecular chaperones may cause the assembly to be trapped at intermediate states instead of transforming into the product, therefore inhibiting the assembly. Consequently, the quantity of molecular chaperones does not follow the intuition that ‘more is better’ for catalyzing assembly, but instead has an optimal molar ratio. Similar phenomena have been reported in biological systems. For example, low content of liposome vesicles can induce α -synuclein aggregation, while high molar ratios inhibit its aggregation^[45]. In the case of RNA-binding proteins like FUS and TDP43, low content of RNA can promote the phase separation of protein and further aggregation, whereas high ratios prevent droplet formation, keeping the proteins dissolved^[46]. It was found that low concentrations of Prostaglandin E2 can promote dendritic cell migration, while high concentrations have the opposite effect^[47]. Therefore, we believe that such dosage-dependent role switching phenomena may be ubiquitous in assembly systems, yet they have not received adequate attention. For instance, extensive studies have demonstrated that liquid-liquid phase separation is closely related to the assembly of proteins^[42, 46, 48]. However, the formation of droplets may either facilitate or inhibit^[46, 49] protein assembly. Studies argue that protein aggregation and the complex coacervation are independent processes^[50]. Therefore, how LLPS affects protein assembly remains elusive. We suggest that for systems involving multicomponent in LLPS, the impact of their dosage on peptide assembly should not be disregarded. Additionally, for drugs that inhibit amyloid aggregation of proteins, the potential risks brought by concentration changes after metabolism should be evaluated. Insufficient inhibitors may keep protein aggregation in the highly toxic oligomeric stage, and residual small amounts of inhibitors may promote aggregation of protein monomers^[51].

3 .

Conclusion

In summary, we have demonstrated how artificial molecular chaperones can serve opposite roles, i.e. catalyst or inhibitor, depending on their dosage in regulating the assembly of peptides. Low dosages of molecular chaperones catalyze peptide assembly into fibrils through multi-step phase separation, while high dosages trap peptides into coacervate intermediates and therefore inhibit assembly. This study provides a clue to elucidate the intricate relationship between phase separation and peptide assembly. When a phase separated system contains multiple components, additives, or impurities, careful examination of their dosage effects on assembly kinetics should not be overlooked. Moreover, this study provides insights into the multifaceted roles chaperones may play in regulating molecular assembly, facilitates the development of chaperone-assisted assembly strategy [24, 42, 43, 52-55] for the construction of complex assembly systems.

Materials and Methods

Detailed materials and methods are included in *SI Appendix*. The fibrillation of peptides was characterized by TEM, CLSM, ThT fluorescence, and CD. Interactions between CMD and peptides were studied by FRET, SPR, and ITC.

Acknowledgements

We thank Junjie Chen (Core Facility of Biomedical Sciences, Xiamen University, Xiamen 361001, PR China) for helpful discussion and assistance in the experiments. This work was supported by the National Natural Science Foundation of China (NSFC) (Nos. 21991130, 21991131, 21971216, 21971217, 22372139, 22250004), the Top-Notch Young Talents Program of China, and the Fundamental Research Funds for the Central Universities of China (No. 20720210007).

Conflict of Interests

The authors declare no competing interests.

Supporting Information

Supporting Information is available from the Wiley Online Library or from the author.

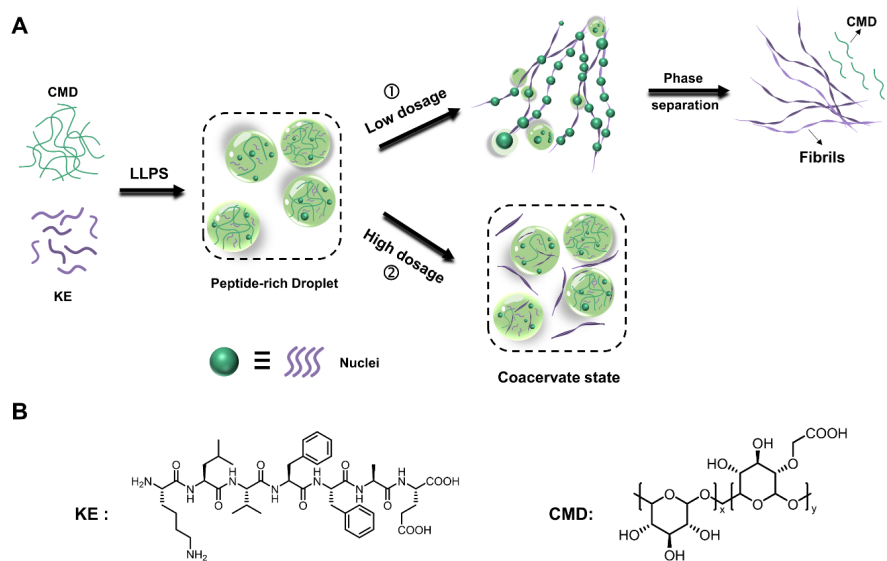
Received: ((will be filled in by the editorial staff)) Revised: ((will be filled in by the editorial staff)) Published online: ((will be filled in by the editorial staff))

References

1. N. J. Van Zee, B. Adelizzi, M. F. J. Mabesoone, X. Meng, A. Aloï, R. H. Zha, M. Lutz, I. A. W. Filot, A. R. A. Palmans, E. W. Meijer, *Nature***2018**, 558, 100.
2. M. Wehner, F. Würthner, *Nat. Rev. Chem.* **2019**, 4, 38.
3. M. F. J. Mabesoone, A. R. A. Palmans, E. W. Meijer, *J. Am. Chem. Soc.***2020**, 142, 19781.
4. M. F. J. Mabesoone, G. M. ter Huurne, A. R. A. Palmans, E. W. Meijer, *J. Am. Chem. Soc.* **2020**, 142, 12400.
5. K. V. Rao, M. F. J. Mabesoone, D. Miyajima, A. Nihonyanagi, E. W. Meijer, T. Aida, *J. Am. Chem. Soc.* **2019**, 142, 598.
6. M. D. Preuss, S. A. H. Jansen, G. Vantomme, E. W. Meijer, *Isr. J. Chem.* **2021**, 61, 622.
7. T. Schnitzer, M. D. Preuss, J. van Basten, S. M. C. Schoenmakers, A. J. H. Spiering, G. Vantomme, E. W. Meijer, *Angew. Chem. Int. Ed.***2022**, 61, e202206738.
8. L. Su, J. Mosquera, M. F. J. Mabesoone, S. M. C. Schoenmakers, C. Muller, M. E. J. Vleugels, S. Dhiman, S. Wijker, A. R. A. Palmans, E. W. Meijer, *Science* **2022**, 377, 213.
9. E. Weyandt, L. Leanza, R. Capelli, G. M. Pavan, G. Vantomme, E. W. Meijer, *Nat. Commun.* **2022**, 13, 248.

10. F. Würthner, *J. Org. Chem.* **2021** , 87, 1602.
11. Y. L. Zhang, S. L. Zhang, H. T. Wu, X. Dong, P. C. Shi, H. Qu, Y. Q. Chen, X. Y. Cao, Z. Q. Tian, X. L. Hu, L. L. Yang, *J. Am. Chem. Soc.***2022** , 144, 19410.
12. P. K. Hashim, J. Bergueiro, E. W. Meijer, T. Aida, *Prog. Polym. Sci.***2020** , 105, 101250.
13. Y. Xue, C. Zhang, T. Lv, L. Qiu, F. Wang, *Angew. Chem. Int. Ed.***2023** , 62, e202300972.
14. W. Wagner, M. Wehner, V. Stepanenko, F. Würthner, *J. Am. Chem. Soc.***2019** , 141, 12044.
15. S. Ogi, K. Sugiyasu, S. Manna, S. Samitsu, M. Takeuchi, *Nat. Chem.***2014** , 6, 188.
16. S. Sarkar, A. Sarkar, A. Som, S. S. Agasti, S. J. George, *J. Am. Chem. Soc.* **2021** , 143, 11777.
17. F. Wang, R. Liao, F. Wang, *Angew. Chem. Int. Ed.* **2023** , 62, e202305827.
18. J. Kang, D. Miyajima, T. Mori, Y. Inoue, Y. Itoh, T. Aida, *Science***2015** , 347, 646.
19. A. Sharko, D. Livitz, S. De Piccoli, K. J. M. Bishop, T. M. Hermans, *Chem. Rev.* **2022** , 122, 11759.
20. A. Sorrenti, J. Leira-Iglesias, A. J. Markvoort, T. F. A. de Greef, T. M. Hermans, *Chem. Soc. Rev.* **2017** , 46, 5476.
21. B. Qin, S. Zhang, Q. Song, Z. Huang, J.-F. Xu, X. Zhang, *Angew. Chem. Int. Ed.* **2017** , 56, 7639.
22. X. Yang, Q. Ji, J. Liu, Y. Liu, *CCS Chem.* **2023** , 5, 761.
23. R. Mitra, K. Wu, C. Lee, J. C. A. Bardwell, *Annu. Rev. Biophys.***2022** , 51, 409.
24. F. H. Ma, C. Li, Y. Liu, L. Shi, *Adv. Mater.* **2020** , 32, e1805945.
25. L. Kleine-Kleffmann, V. Stepanenko, K. Shoyama, M. Wehner, F. Würthner, *J. Am. Chem. Soc.* **2023** , 145, 9144.
26. R. Mitra, V. V. Gadkari, B. A. Meinen, C. P. M. van Mierlo, B. T. Ruotolo, J. C. A. Bardwell, *Nat. Commun.* **2021** , 12, 851.
27. A. P. Capaldi, C. Kleanthous, S. E. Radford, *Nat. Struct. Biol.***2002** , 9, 209.
28. F. Stull, P. Koldewey, J. R. Humes, S. E. Radford, J. C. A. Bardwell, *Nat. Struct. Mol. Biol.* **2015** , 23, 53.
29. K. Wu, T. C. Minshull, S. E. Radford, A. N. Calabrese, J. C. A. Bardwell, *Nat. Commun.* **2022** , 13, 4126.
30. P. Koldewey, F. Stull, S. Horowitz, R. Martin, J. C. A. Bardwell, *Cell* **2016** , 166, 369.
31. S. Zhao, Y. Song, L. Xu, H. Hu, J. Wang, F. Huang, L. Shi, *Macromol. Biosci.* **2023** , DOI: 10.1002/mabi.202300205, 2300205.
32. F.-H. Ma, Y. An, J. Wang, Y. Song, Y. Liu, L. Shi, *ACS Nano***2017** , 11, 10549.
33. F. Ma, X. Wu, A. Li, L. Xu, Y. An, L. Shi, *Angew. Chem. Int. Ed.***2021** , 60, 10865.
34. X. Wu, F. Ma, B. B. Pan, Y. Zhang, L. Zhu, F. Deng, L. Xu, Y. Zhao, X. Yin, H. Niu, X. C. Su, L. Shi, *Angew. Chem. Int. Ed.* **2022** , 61, e202200192.
35. Z.-C. Lei, X. Wang, H. Qu, C. Zhou, Z. Li, L. Yang, X. Cao, Z.-Q. Tian, *Sci. Sin. Chim.* **2020** , 50, 1781.
36. Y. Wang, H. X. Lin, L. Chen, S. Y. Ding, Z. C. Lei, D. Y. Liu, X. Y. Cao, H. J. Liang, Y. B. Jiang, Z. Q. Tian, *Chem. Soc. Rev.***2014** , 43, 399.
37. Y. Wang, Y. Sun, P. Shi, M. M. Sartin, X. Lin, P. Zhang, H. Fang, P. Peng, Z. Tian, X. Cao, *Chem. Sci.* **2019** , 10, 8076.

38. N. J. Greenfield, *Nat. Protoc.* **2006** , 1, 2876.
39. H. LeVine, 3rd, *Protein Sci.* **1993** , 2, 404.
40. S. A. Semerdzhiev, M. A. A. Fakhree, I. Segers-Nolten, C. Blum, M. Claessens, *ACS Chem. Neurosci.* **2022** , 13, 143.
41. M. A. A. Fakhree, I. S. Nolten, C. Blum, M. Claessens, *J. Phys. Chem. Lett.* **2018** , 9, 1249.
42. C. Yuan, Q. Li, R. Xing, J. Li, X. Yan, *Chem* **2023** , 9, 1.
43. C. Yuan, R. Xing, J. Cui, W. Fan, J. Li, X. Yan, *CCS Chem.***2023** , DOI: 10.31635/cc-schem.023.202302990, 1.
44. T. Ikenoue, Y. H. Lee, J. Kardos, H. Yagi, T. Ikegami, H. Naiki, Y. Goto, *Proc. Natl. Acad. Sci. USA* **2014** , 111, 6654.
45. C. Galvagnion, A. K. Buell, G. Meisl, T. C. Michaels, M. Vendruscolo, T. P. Knowles, C. M. Dobson, *Nat. Chem. Biol.***2015** , 11, 229.
46. S. Maharana, J. Wang, D. K. Papadopoulos, D. Richter, A. Pozniakovsky, I. Poser, M. Bickle, S. Rizk, J. Guillén-Boixet, T. M. Franzmann, M. Jahnel, L. Marrone, Y.-T. Chang, J. Sternecker, P. Tomancak, A. A. Hyman, S. Alberti, *Science* **2018** , 360, 918.
47. G. Diao, J. Huang, X. Zheng, X. Sun, M. Tian, J. Han, J. Guo, *Int. J. Mol. Med.* **2020** , 47, 207.
48. M. C. Hsieh, D. G. Lynn, M. A. Grover, *J. Phys. Chem. B***2017** , 121, 7401.
49. G. G. Moreira, C. M. Gomes, *J. Neurochem.* **2023** , 166, 76.
50. Y. Lin, Y. Fichou, Z. Zeng, N. Y. Hu, S. Han, *ACS Chem. Neurosci.***2020** , 11, 615.
51. J. Yang, A. J. Dear, Q. Q. Yao, Z. Liu, C. M. Dobson, T. P. J. Knowles, S. Wu, S. Perrett, *Nanoscale* **2020** , 12, 18663.
52. D. Yao, Y. Zhang, X. Zhou, X. Sun, X. Liu, J. Zhou, W. Jiang, W. Hua, H. Liang, *Proc. Natl. Acad. Sci. USA* **2023** , 120, e2219034120.
53. Y. Jiao, J. F. Stoddart, *Tetrahedron* **2022** , 126, 133065.
54. W. Zhi, Z. Pu, C. Ma, K. Liu, X. Wang, J. Huang, Y. Xiao, Y. Yan, *ACS Nano* **2021** , 15, 19621.
55. Z.-C. Lei, X. Yin, X. Wang, G. Ke, X. Cao, C. Fan, C. J. Yang, H. Liang, Z.-Q. Tian, *Giant* **2020** , 1, 100008.



Scheme 1. Schematic diagram of the KE assembly chaperoned by CMD. (A) CMD catalyzed KE assembly through multi-step phase separation at low dosage, while it inhibited the KE assembly at high dosage. (B) The molecular structures of KE and CMD.

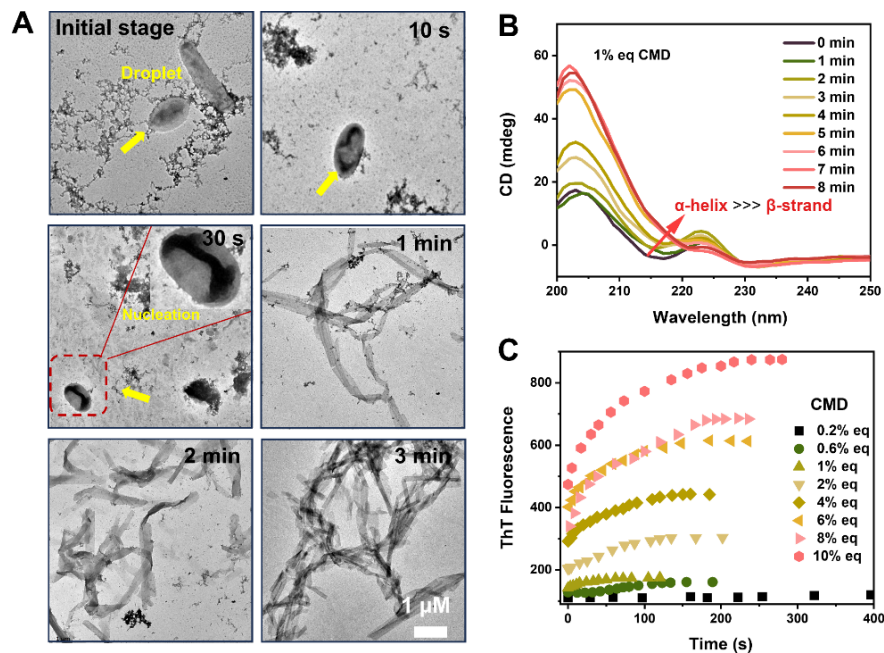


Figure 1. Using TEM, circular dichroism spectroscopy, and fluorescence probe to monitor the KE assembly process promoted by CMD. (A) TEM images demonstrated the fibrillation process of KE (100 μ M) when incubated with CMD (1 μ M). (B) Time-dependent CD spectra for monitoring the conformational switching of KE from α -helix to β -strand upon adding CMD. (C) Time-dependent fluorescence spectra for monitoring the assembly of KE into β -sheets promoted by different contents of CMD.

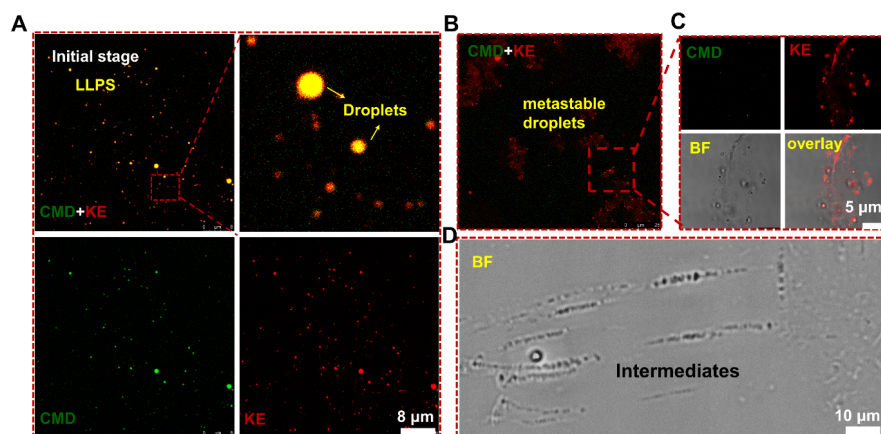


Figure 2. CLSM images of the assembly process of KE promoted by CMD. (A) the CMD and KE formed coacervate droplets through LLPS. (B-C) the droplets functioned as nucleating centers, enabling the formation of thermodynamically favorable fibrils following Ostwald's step rule.^[42] (D) Coalescence and fusion of the droplets were observed during the fibrillation process.

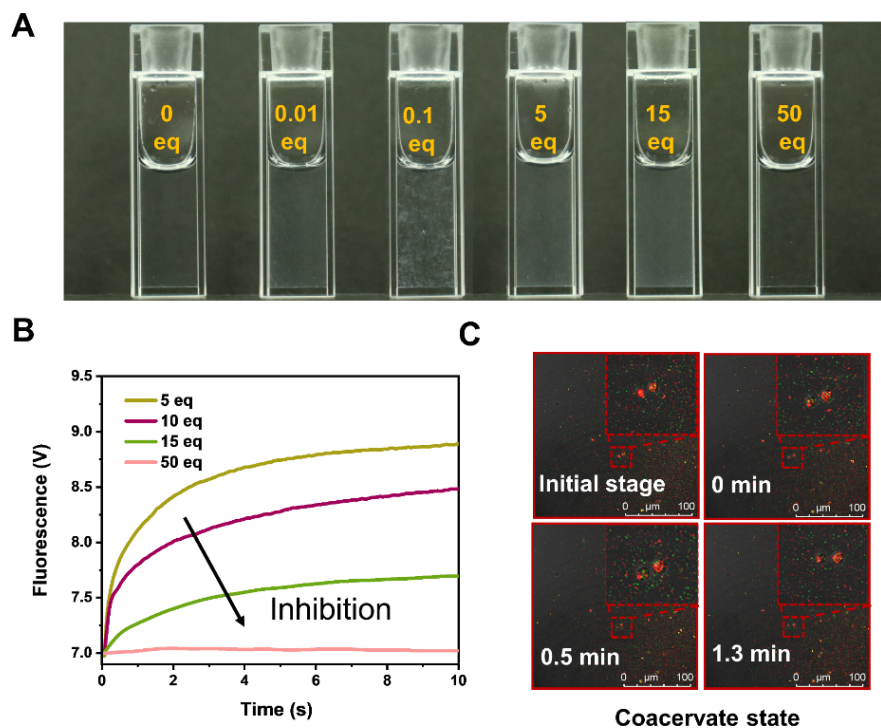


Figure 3. High dosage of CMD inhibit the assembly of KE. (A) Images of KE solutions that incubated with different equivalents of CMD. White fibrils were clearly observed in the solution with 0.1 equivalent of CMD. (B) Fitted plots of the assembly kinetics when the KE (100 μ M) solutions were incubated with different contents of CMD. (C) CLSM images demonstrated that the coacervates formed by KE and 50 equivalents of CMD remained stable.

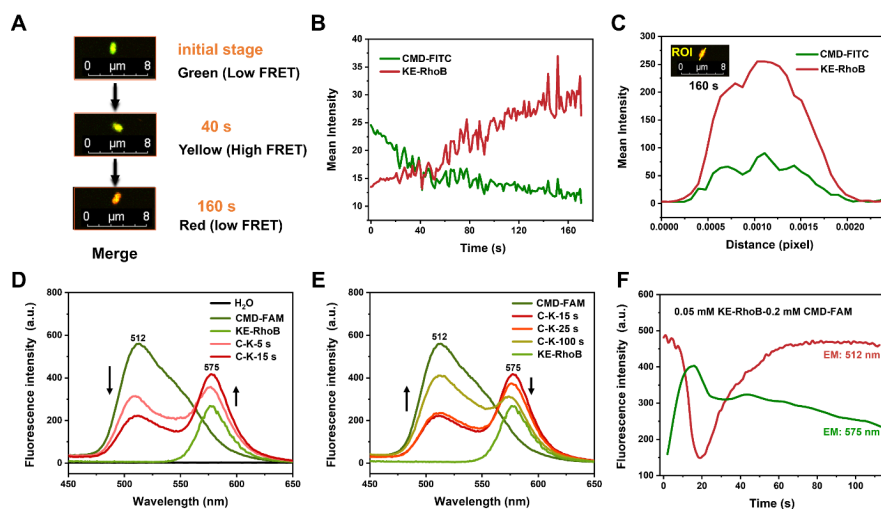


Figure 4. In-situ monitoring the evolution of interactions between KE and CMD. (A) Images of a selected region at different time points. (B) The time-dependent fluorescence co-localization analysis of the selected region. (C) The plot-line analysis of the selected region at 160 s. (D) The mixing of CMD-FAM and KE-RhoB resulted in an instant rising of emission at 575 nm, accompanied by a decline of emission at 512 nm, indicating the FRET effect between these two components. [CMD-FAM] = 0.2 mM, [KE-RhoB] = 0.05 mM. (E) As the assembly progressed, the emission at 575 nm declined while the emission at 512 nm gradually recovered, indicating the attenuation of FRET. (F) The evolutions of emission intensities at 512 nm and 575 nm.

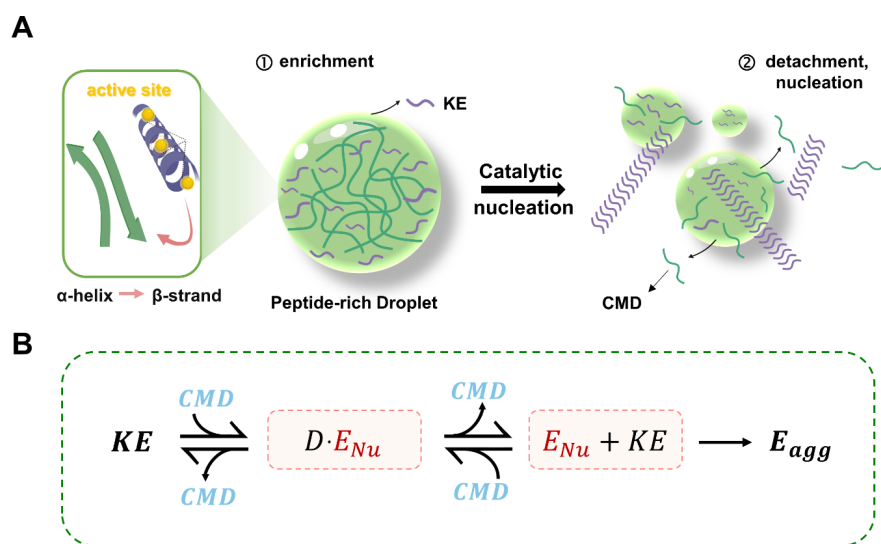


Figure 5. Schematic representation of the catalytic assembly mechanism of CMD in promoting the assembly of KE. (A) The complexation of CMD and KE molecules resulted in the formation of coacervate droplets, and promoted the conformational transition of peptides from α -helix to β -strand. Then β -strand monomers assembled into fibrils by expelling CMD through phase separation. (B) The proposed assembly equation of KE catalyzed by CMD.

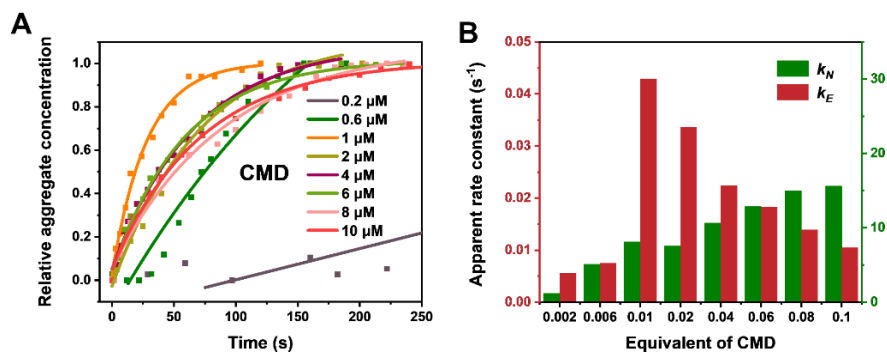


Figure 6. Kinetic analysis of the assembly of KE regulated by CMD. (A) A fit plot of the KE (100 μ M) assembly kinetics with varied contents of CMD. (B) The apparent nucleation rate constant k_N and apparent elongation rate constant k_E for the assembly of KE with varied equivalents of CMD.

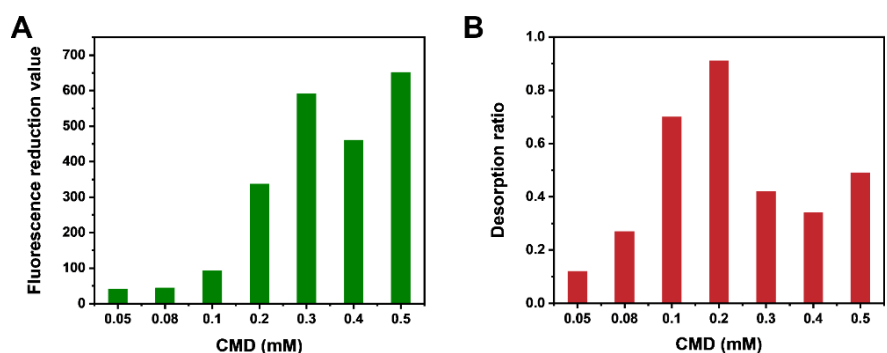


Figure 7. Further analysis of the changes of emission intensity at 512 nm during the FRET experiments, revealing the details of the adsorption and desorption of KE-RhoB. The KE-RhoB concentration was kept constant (0.05 mM) with the increase of the CMD-FAM concentration from 0.05 to 0.5 mM. (A) The fluorescence reduction values at 512 nm correspond to the maximum amount of KE-RhoB adsorbed by CMD-FAM at the initial stage. (B) The desorption ratio is the degree of recovery of emission at 512 nm, corresponding to the regeneration of CMD-FAM.

An artificial chaperone can serve opposite roles, a catalyst at low dosage while an inhibitor at high dosage, in regulating the supramolecular polymerization of peptides. This system undergoes a cascading phase separation process, and the interplay and evolution of electrostatic and hydrophobic interactions between chaperones and peptides are the keys to achieving these processes.

Keywords: artificial chaperone, catassembly, supramolecular polymerization, peptide assembly

Wang Li,^a Yang Zhou,^a Sheng He,^a Congsen Wang,^a Peichen Shi,^a Suixu Li,^a Xinchang Wang,^b Liulin Yang,^{*a} Xiaoyu Cao,^{*a} and Zhongqun Tian^a

An Artificial Chaperone Serves a Dual Role in Regulating the Assembly of Peptides through Phase Separation

